ELSEVIER

European Polymer Journal 37 (2001) 2273–2279

EUROPEAN POLYMER JOURNAL

www.elsevier.com/locate/europolj

Synthesis and characterization of poly(*n*-hexyl methacrylate) in three-component microemulsions

Issa Katime [a,*], Jesús Arellano [b], Eduardo Mendizábal [b], Jorge Puig [b]

[a] *Grupo de Nuevos Materiales, Departamento de Química Física, Campus de Lejona, Universidad del País Vasco, Apartado 644, Bilbao 48080, Spain*

[b] *Departamento de Química, CUCEI, Universidad de Guadalajara, M. García Barragán, 1451, Guadalajara, Jalisco 44430, Mexico*

Received 14 August 2000; received in revised form 10 May 2001; accepted 15 May 2001

Abstract

The polymerization of *n*-hexyl methacrylate in three-component microemulsions stabilized with dodecyltrimethylammonium bromide is examined here as a function of the concentration of a water-soluble (V-50) and an oil-soluble (2, 2-azobisisobutyronitrile) initiators, of monomer concentration in the parent microemulsions and temperature. At high temperatures and high initiator concentrations, only two reaction rate intervals are observed; however, at low temperatures and low initiator concentrations, a slow rate period is observed whose duration increases as the temperature or the initiator concentration diminish. This slow rate period appears to be due to homogeneous nucleation. Particle size of polymer particles is small and remains constant throughout the reaction. Molar mass is high and also remains constant throughout the reaction.

Keywords: Microemulsion; Polymerization; Poly(*n*-hexyl methacrylate); Particle size; Quasielastic light scattering

1. Introduction

Oil-in-water microemulsion polymerization is a novel process that allows the synthesis with fast reaction rates of colloidal nanoparticles of high molar mass polymers dispersed in aqueous media [1–5]. Up to the late 1980s, most work on o/w microemulsion polymerization was performed in four- or five-component systems – monomer, water, surfactant, an alcohol cosurfactant and/or electrolytes [6–20]. Jayakrishnan and Shah [21] made the first report on polymerization in a cosurfactant-free microemulsion using a mixture of surfactants. Later, Ferrick et al. [22] and Pérez-Luna et al. [23] reported the polymerization in three-component microemulsions (monomer, water and a single surfactant). Since then, scores of papers on the polymerization of vinyl and acrylic monomers in three-component microemulsions have been forwarded [24–40].

Even though, microemulsion polymerization has not been scaled up to industrial level, mainly because the low ratio of polymer produced to surfactant employed, efforts to overcome this problem have been recently reported [41–44]. Hence, it is important to understand fully the process of microemulsion polymerization.

In this paper we report the polymerization of *n*-hexyl methacrylate (HeMA) in three-component microemulsions stabilized with dodecyltrimethylammonium bromide (DTAB) as a function of initiator type and concentration, monomer concentration in the parent microemulsions and temperature. Latexes, characterized by quasielastic light scattering (QLS) and gel permeation chromatography (GPC), contain small particles ($D_P < 30$ nm) of high molar mass poly(HeMA).

2. Experimental section

DTAB (99% pure from Aldrich) was recrystallized from an ethanol/ethyl ether mixture (50:50 v/v). HeMA (99% pure from Scientific Polymer Products) was passed

* Corresponding author. Tel.: +34-94-601-5441/2531; fax: +34-94-464-8500.

E-mail address: qfpkaami@lg.ehu.es (I. Katime).

0014-3057/01/$ - see front matter
PII: S0014-3057(01)00122-7

through a DE-HIBIT 100 column (SPP) to remove the inhibitor before polymerization. 2,2′-Azobis (2-amidinopropane) hydrochloride (V-50) from Wako was recrystallized from methanol. 2,2-Azobisisobutyronitrile (AIBN) was 99% pure from Merck. Doubly distilled and deionized water was used. HPLC-grade tetrahydrofurane (Merck) was used as the mobile phase in GPC.

Phase diagrams at 25°C and 60°C were obtained by titrating aqueous solutions of DTAB with HeMA until turbidity and phase separation were detected by the naked eye. To determine more accurately phase boundaries, samples with compositions slightly below and above the phase boundaries determined by titration were prepared by weighing all the components in vials and immersed in a water bath at 25°C or 60°C for equilibration. One-phase samples were examined through cross-polarizers to detect for streaming or static birefringence.

Polymerization kinetics was followed in a 25 ml glass dilatometer immersed in a thermostated water bath. Microemulsions for polymerization were prepared by dissolving the surfactant in water ($DTAB/H_2O = 15/85$ by weight) and adding the specified amount of monomer (1–4 wt.%) – a small amount of water was reserved for preparing the initiator solution when V-50 was employed or a small amount of monomer when AIBN was used. Except when indicated, initiator concentrations are given in weight percent with respect to monomer. Before initiating the reaction, the microemulsion in the dilatometer was sparged with argon at room temperature for about 45 min and heated to the temperature of reaction before injecting the initiator solution through a septum. Conversion as a function of time was estimated by measuring the change in height of the liquid in the capillary tube of the dilatometer, assuming that the volume change is directly proportional to conversion. The dilatometer was calibrated by assigning the final height in the capillary tube to the final conversion determined by gravimetry.

Particle size was measured in an AMTEC QLS instrument equipped with a BI-9000AT correlator and a He–Ne laser ($\lambda = 632.8$ nm). Intensity correlation data were analyzed by the method of cumulants to provide the average decay rate, $\langle \Gamma \rangle (= q^2 D)$, where q is the scattering vector and D is the diffusion coefficient. The measured diffusion coefficients were represented in terms of apparent radii by using Stokes law and assuming the solvent has the viscosity of water. Latexes were diluted up to 250 times to minimize interactions and filtered through 0.2 μm Millipore Acrodisc-13 filters to eliminate dust before QLS measurements.

Average molar masses were measured in a HPLC apparatus consisting of a Knauer HPLC64 injection pump, a Rheodyne 7125 manual injector, a Knauer differential refractive index detector, two PLGEL-mixed-C chromatographic columns, a Polymer Laboratories PL-LALS interface and a PC-486 computer equipped with a PL Caliber, GPC/SEC software.

3. Results

Fig. 1 reports partial phase diagrams at 25°C and 60°C of mixtures of HeMA, DTAB and water. A one-phase region forms at the water-DTAB side of the ternary phase diagram. The extension of the one-phase region increases with temperature. Below 20 wt.% DTAB and within the one-phase region, samples are transparent, highly conductive, nonbirefringent (when examined through cross-polarizers) and exhibit low viscosity. As the concentration of DTAB is increased, samples become more viscous and acquire a bluish tinge, although they remain nonbirefringent. Only those one-phase transparent or bluish samples that did not exhibit birefringence were considered microemulsions.

Fig. 2 reports conversion versus time for the microemulsion polymerization of HeMA initiated at 60°C with different V-50 concentrations. Conversions near 100% are achieved at all initiator concentrations examined here; moreover, reaction rates increase with initiator concentration (inset in Fig. 2). It is noteworthy that an initial slow period is observed at low V-50 concentrations with a duration that increases with decreasing V-50 concentration. At sufficiently high V-50 concentration, this slow period appears to vanish. At the higher levels of V-50 concentrations examined here, only two reaction rate intervals are detected (inset in Fig. 2), which is typical of microemulsion polymerization [3–5]. However, an additional interval appears at low V-50 concentrations due to the occurrence of the slow-rate period. Not withstanding, the maximum reaction rate occurs at same conversion, regardless of initiator concentration.

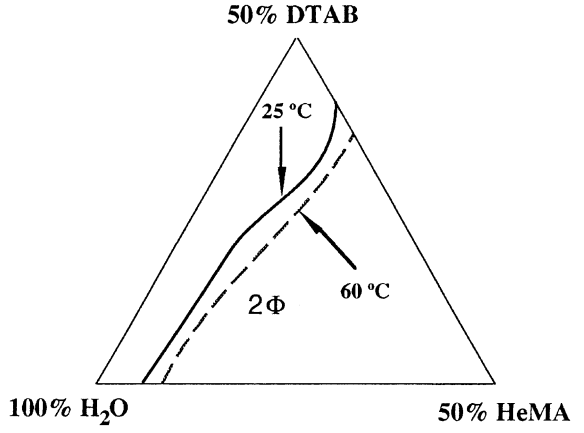

Fig. 1. Partial phase diagrams of water, HeMA and DTAB. The one-phase microemulsion region is bound by the water–DTAB side of the diagram and the solid line (25°C) or the broken line (60°C). Also, a neighboring two-phase emulsion (2ϕ) region is depicted in the diagram.

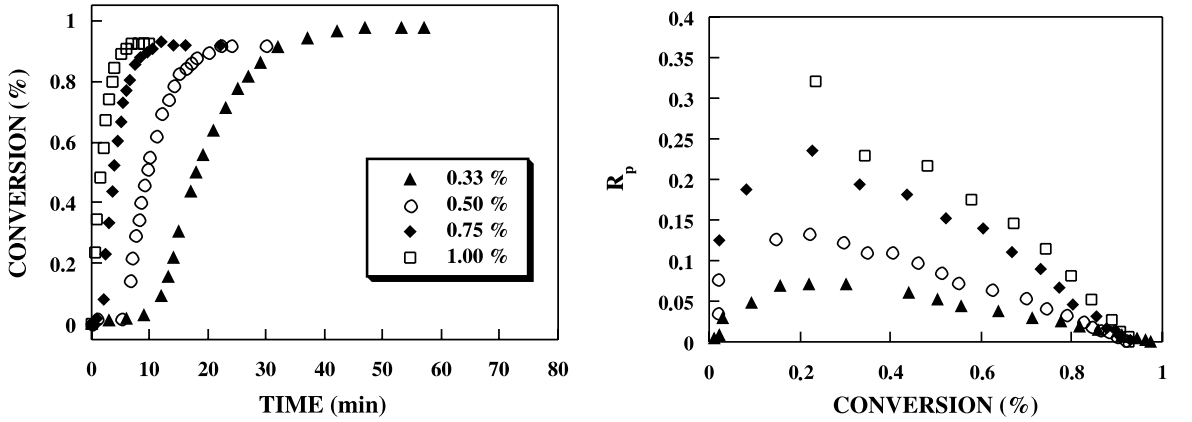

Fig. 2. Conversion versus time for the microemulsion polymerization of HeMA initiated at 60°C as a function of V-50 concentration given in weight percent with respect to monomer content. Inset: Reaction rate versus concentration as a function of V-50 concentration.

Fig. 3 depicts conversion as a function of time for the polymerization of microemulsions containing different monomer concentrations, initiated with identical V-50 concentration (0.02 w/w microemulsion). Again, an initial slow period followed by a rapid increase in reaction rate is observed. Conversions near 100% are obtained in all cases in less than 25 min. Notice, moreover, than data of conversion versus time nearly overlap, indicating that reaction rate is practically independent of the initial monomer content in the parent microemulsions.

The effect of temperature on the polymerization of 4 wt.% HeMA microemulsions initiated with 0.5% V-50 is reported in Fig. 4. As expected, reaction rates increase rapidly with increasing temperature; moreover, with the exception of the 40°C experiment, conversions near 100% are obtained. A slow-rate period is also observed at low conversions whose duration diminishes rapidly with increasing reaction temperature. At the lowest temperature examined, the slow period lasted more than 5 h without any evidence of an upturn in reaction rate. Moreover, the plot of the logarithm of maximum reaction rate versus $T-1$ is linear. From the slope of the Arrhenius plot, an activation energy of 101.7 kJ/mol was estimated.

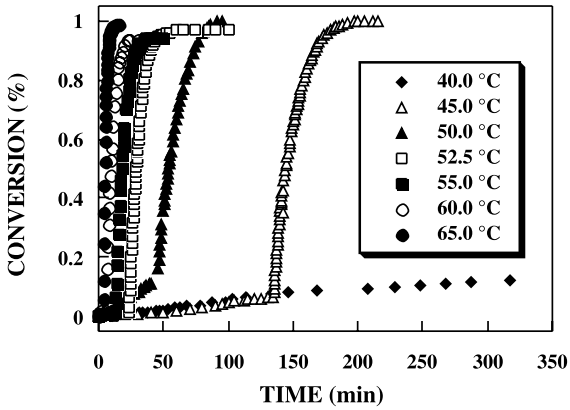

Fig. 4. Conversion versus time for the microemulsion polymerization of HeMA initiated with 0.5% V-50 at different temperatures.

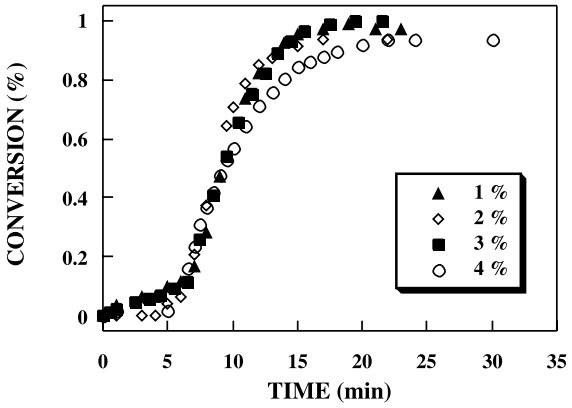

Fig. 3. Conversion versus time for the polymerization of HeMA in microemulsions containing different initial monomer concentrations. Reactions were carried out at 60°C and 0.02 wt.% V-50.

The polymerization kinetics of HeMA in DTAB microemulsions initiated with an oil-soluble initiator, AIBN, is reported in Fig. 5. Reaction rates increase with AIBN concentration, although they are much slower than those determined with V-50; nevertheless, conversions close to 100% are obtained at all AIBN concentrations. A retardation period is also observed here,

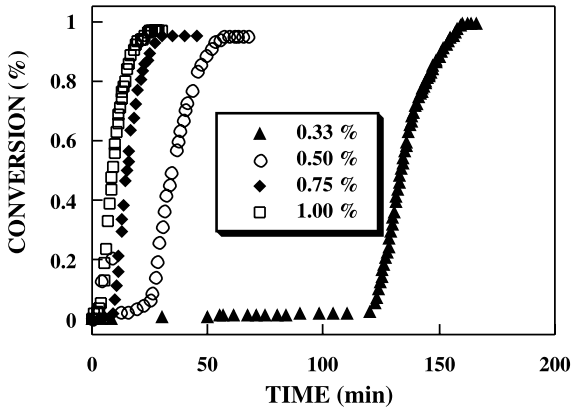

Fig. 5. Conversion versus time for the microemulsion polymerization of HeMA initiated at 60°C as a function of AIBN concentration given in weight percent with respect to monomer content.

whose duration augments with decreasing AIBN concentration. In fact, for the lowest AIBN concentration examined here, the retardation period lasted more than 2 h, before reaction rate speeded up.

Particle size and molecular weight were followed as a function of conversion for the polymerization of 4 wt.% HeMA in a 15/85 DTAB/water microemulsion initiated with 0.5% V-50 at 60°C. Results reported in Table 1 show that both particle size (D_P) and average molar mass remain constant throughout the reaction, except at low conversions where MW is smaller. This behavior appears to be typical of the polymerization of water-insoluble monomers in o/w microemulsion media [4]. Particle size and average molar masses could not be obtained at conversions smaller than 20% due to the small amount of polymer isolated and because samples become unstable upon dilution with water for QLS measurements.

The effects of initiator concentration, initial monomer content and temperature on final particle size and average molar masses are compiled in Tables 2–4. Both particle size and average molar mass are independent of V-50 concentration (Table 2). However, particle size decreases whereas average molar mass increase with increasing HeMA content (Table 3). This is an unexpected result inasmuch as the overall concentration of initiator was the same in these reactions. Finally, particle size increases with increasing temperature whereas molar masses are fairly insensitive to the reaction temperature (Table 4).

Table 1
Final particle size and weight-average molar mass for different conversions during the microemulsion polymerization of 4 wt.% HeMA initiated at 60°C with 0.5% V-50

Conversion (%)	D_p (nm)	$M_W \times 10^{-6}$ (g/mol)
20	16.2	3.0
45	15.6	4.7
60	16.1	4.4
93.5	15.8	4.5

Table 2
Final particle size and weight-average molar mass for different V-50 concentrations during the microemulsion polymerization of 4 wt.% HeMA initiated at 60°C

[V-50] (wt.%)	D_p (nm)	$M_W \times 10^{-6}$ (g/mol)
0.33	15.3	3.7
0.50	15.8	4.5
0.75	15.6	4.6
1.00	15.3	3.9

Table 3
Final particle size and weight-average molar mass for the polymerization of HeMA in microemulsions containing different monomer content[a]

[HeMA] (wt.%)	D_p (nm)	$M_W \times 10^{-6}$ (g/mol)
1	27	1.31
2	22	2.8
3	18.6	3.9
4	15.8	4.5

[a] Reactions were carried out at 60°C with 0.02 wt.% V-50 (with respect to overall system).

Table 4
Final particle size and weight-average molar mass for the microemulsion polymerization of 4 wt.% HeMA initiated with 0.5% V-50 at different temperatures

T (°C)	D_p (nm)	$M_W \times 10^{-6}$ (g/mol)
50	14.1	3.8
55	14.5	3.8
60	15.8	4.4
65	18.75	–

4. Discussion and conclusions

One-phase transparent microemulsions of HeMA, DTAB and water were found at 25°C and 60°C at the water-rich corner of the phase diagram (Fig. 1). The one-phase region increases with temperature. The extent of the one-phase region is slightly smaller than those found for DTAB microemulsions of methyl and butyl methacrylate [29,34], probably because of the less hydrophilic nature of HeMA. Microemulsions are optically transparent, nonbirefringent, highly conductive and have low

viscosities for concentrations smaller than 20 wt.% DTAB. For higher concentrations, samples are also transparent, nonbirefringent but highly viscous. At some compositions, microemulsions exhibit a blue tinge.

The polymerization of HeMA in three-component microemulsions is fast and conversions close to 100% are achieved in a few minutes (Figs. 2–5). The initially transparent o/w microemulsions develop a bluish tinge at the onset of particle nucleation and become increasingly turbid as the polymerization is carried out due to particle growth and the increase in refractive index contrast between the particles and the aqueous phase as monomer changes into polymer. Final lattices range from bluish to opaque, depending on microemulsion composition and polymerization conditions. The lattices have remained stable respect to coagulation for months.

Faster reaction rates are obtained with increasing V-50 (Fig. 2) or AIBN concentration (Fig. 5) because the larger free radical flux induces a more rapid particle nucleation rate that speeds up the reaction. However, reaction rates are faster with V-50 than with AIBN. This is a consequence of the differences in decomposition rates of the two initiators and of the concentrations employed. V-50 decomposes about 30 times faster than AIBN at 60°C [45] and since the concentrations used of both initiator are about the same (in mole of initiator per mole of HeMA), it is expected much faster reaction rates with V-50 than with AIBN. However, with both initiators, conversions close to 100% are obtained.

On the other hand, reaction rates and final conversions appear to be insensible to the initial monomer content in the parent microemulsions. However, the overall concentration of initiator was the same (0.02 w/w microemulsion). Hence, free radical flux rate is the same in all cases, which should lead to similar nucleation rates.

Temperature has a strong effect on reaction rate and conversion (Fig. 4) because both the initiator decomposition rate constant (k_I) and the VA propagation rate constant (k_p) increase with increasing temperature. Reaction rate follows an Arrhenius kinetics, which is typical of microemulsion polymerization [4], with an activation energy of 101.7 kJ/mol.

Typically, in microemulsion polymerization only two reaction-rate intervals are detected. The polymerization rate first increases rapidly because of the fast particle nucleation rate and then it decreases steadily after passing through a maximum, because monomer concentration within the particles begins to diminish as a result of the disappearance of the microemulsion droplets [4]. This fact does not contravene the continuous particle nucleation mechanism, which has been proposed for o/w microemulsion polymerization [4,17,18,46]. In fact, the large amount of surfactant present in microemulsion polymerization allows the nucleation and stabilization of new particles throughout the reaction. However, the rate of decrease of monomer in the particles should be faster than the rate of particle nucleation during the second interval so a net decrease in polymerization rate is observed [46].

Here, two reaction rate intervals are detected at high initiator concentrations and reaction temperatures. However, as temperature and/or initiator concentration is decreased, a slow-rate or retardation period is observed (Figs. 2–5). Clearly, this retardation period is not an artifact inasmuch as the inhibitor was removed from monomer and the microemulsion systems purged exhaustively with nitrogen before initiating the reaction. As seen in Figs. 2–5, a "slow regime" occurs up to 5–10% conversion, depending on reaction conditions, after which reaction rate speeds up. This retardation period has also been observed in the microemulsion polymerization of styrene [15,23] and of methyl methacrylate [46]. However, Morgan et al. [36] did not observed a retardation period in the polymerization initiated with V-50 of HeMA in microemulsions stabilized with a mixture of two cationic surfactants, DTAB and DDAB (didodecyldimethylammonium bromide).

According to studies of the emulsion polymerization of styrene [47], the induction period caused by oxygen is inversely proportional to the amount of initiator. Hence, the product of initiator concentration and the induction (or retardation) time should be constant for this process. Table 5 shows that the product of these two parameters increases with initiator concentration with both V-50 and AIBN. Furthermore, the inhibition constant of oxygen is very large and so, oxygen should only inhibit and not retard the polymerization. Hence, the retardation period cannot be attributed to oxygen.

Bleger et al. [46] suggested that the slow increase in conversion for the microemulsion polymerization of methyl methacrylate may be due to homogeneous nucleation, whereas the speed up in reaction rate involves micellar nucleation which is determined by capture of radicals by microemulsion droplets (micellar entry mechanism). In fact, they showed by transmission electron microscopy, an increase in particle size and number density of particles after the slow period has ended. Some evidence provided here support this hypothesis. Figs. 2 and 5 show the same trends reported by Bleger et al. [46], i.e., the duration of the slow rate period

Table 5
Duration of the slow-rate period for different concentrations of V-50 or AIBN concentration, and the product of the slow-rate period and the initiator concentration

[V-50] (%)	Time (min)	[V-50] × t	[AIBN] (%)	Time (s)	[AIBN] × t
1.00	0	0	1.00	3	3.0
0.75	1	0.75	0.75	9	6.75
0.50	5	5	0.50	22	11.0
0.33	9	9	0.33	120	39.0

decreases with increasing initiator concentration, and it is longer for the oil-soluble initiator. Moreover, as shown in Table 5, the increase in the slow period with decreasing initiator concentration cannot be attributed to a retardation effect. Also, the increase in the slow-rate period with decreasing temperature can be attributed to the smaller free radical flux which induces homogeneous nucleation. Finally, data in Fig. 3 shows that the slow-rate period is practically the same for the polymerization of microemulsions with different monomer content but initiated with the same overall V-50 concentration. Inasmuch as the monomer concentration in the aqueous phase is the same regardless of the initial monomer content in these microemulsions and since the same free radical flux was employed, the fact that the slow rate period is the same, support the argument of homogeneous nucleation at low conversions. Unfortunately, TEM pictures of the latexes were not available to verify this hypothesis. The size polydispersity index (D_w/D_n), obtained from QLS data, remains fairly constant after 20% conversion (1.15–1.25, depending on monomer concentration and temperature). However, no QLS measurements were possible for conversion lower than $\approx$15%, due to emulsification of the latex upon dilution with water, which is necessary to minimize particle–particle interactions.

Of course, the slow rate period can be due to a retardation agent present as an impurity. However, it was not possible to test this hypothesis inasmuch as no chemical analysis on the purified monomer and DTAB were performed.

Within the experimental error, the maximum reaction rate occurs at similar conversions ($x_{max} \approx 35 \pm 2\%$) regardless of the initiator concentration (inset in Fig. 2), HeMA concentration (not shown) or reaction temperature. Morgan et al. [36] also reported a unique value for the conversion where maximum reaction rate occurs. It is noteworthy that for the microemulsion polymerization of several other monomers, x_{max} does not depend on the level of initiator or monomer concentration [13,28,29,34–36].

In microemulsion polymerization, chain transfer to monomer usually controls chain termination events [28,29,34–36,39–41]. In the microemulsion polymerization of HeMA in three-component microemulsion stabilized with DTAB because MW does not seems to be effected by changes in initiator concentration and reaction temperature, it is concluded that chain transfer to monomer controls the molar mass of the polymer.

Acknowledgements

The authors thanks the Departamentos de Industria y Educación, Universidades e Investigación del Gobierno Vasco and the University of Basque Country for their financial support. We also acknowledge the support by CONACYT through grant number 28262U.

References

[1] Candau F. In: Mark HF, Bikales NM, Overberger CG, Menges G, editors. Encyclopedia of polymer science and engineering, vol. 9. New York: Wiley; 1987.
[2] Dunn AS. In: Eastwood GC, Ledwith A, Sigwalt P, editors. Comprehensive polymer science. New York: Pergamon; 1988.
[3] Antonieti M, Basten R, Lohmann S. Macromol Chem Phys 1995;196:441.
[4] Katime I, Mendizábal E, Puig JE. Recent Res Devel Polym Sci 1997;1:271.
[5] Capek I. Adv Colloid Int 1999;80:85.
[6] Atik SS, Thomas KJ. J Am Chem Soc 1981;103:4279.
[7] Atik SS, Thomas KJ. J Am Chem Soc 1982;104:5868.
[8] Atik SS, Thomas KJ. J Am Chem Soc 1983;105:4515.
[9] Gan LM, Shew CH, Friberg SE. J Macromol Chem A 1983;19:739.
[10] Johnson PL, Gulari EJ. J Polym Sci Polym Chem Ed 1984;22:3967.
[11] Grätzel CK, Jirousek M, Grätzel M. Langmuir 1986;2:292.
[12] Kuo PL, Turro NJ, Tseng C, El-Aasser MS, Vanderhoff JW. Macromolecules 1987;20:1216.
[13] Guo JS, El-Aasser MS, Vanderhoff JW. J Polym Sci Polym Chem Ed 1989;27:691.
[14] Schauber C, Riess G. Makromol Chem 1989;190:725.
[15] Feng L, Ng KYS. Macromolecules 1990;23:1048.
[16] Feng L, Ng KYS. Colloids Surf 1991;53:349.
[17] Guo JS, Sudol ED, Vanderhoff JW, El-Aasser MS. J Polym Sci Polym Chem Ed 1992;30:691.
[18] Guo JS, Sudol ED, Vanderhoff JW, El-Aasser MS. J Polym Sci Polym Chem Ed 1992;30:703.
[19] Gan LM, Chew CH, Lye I, Ma L, Li G. Polymer 1993;34:3860.
[20] Full AP, Kaler EW, Arellano J, Puig JE. Macromolecules 1996;30:123.
[21] Jayakrishnan A, Shah DO. J Polym Sci Polym Chem Lett 1984;22:31.
[22] Ferrick MR, Murtagh J, Thomas JK. Macromolecules 1989;22:1515.
[23] Pérez-Luna VH, Puig J, Castaño VM, Rodríguez BE, Murthy AK, Kaler EW. Langmuir 1990;6:1040.
[24] Antonietti M, Bremser W, Müschenborn D, Rosenauer C, Schupp B, Schmidt M. Macromolecules 1991;24:6636.
[25] Texter J, Oppenheimer L, Minter JR. Polym Bull 1992;27:487.
[26] Full AP, Puig JE, Gron LU, Kaler EW, Minter JR, Mourey TH, Texter J. Macromolecules 1992;25:5157.
[27] Gan LM, Chew CH, Lee KC, Ng SC. Polymer 1993;34:3064.
[28] Puig JE, Pérez-Luna VH, Pérez-González M, Macías ER, Rodríguez BE, Kaler EW. Colloid Polym Sci 1993;271:114.

[29] Rodríguez-Guadarrama LA, Mendizábal E, Puig JE, Kaler EM. J Appl Polym Sci 1993;48:775.
[30] Gan LM, Chew CH, Ng SC, Loh SE. Langmuir 1993; 9:2799.
[31] Capek I, Potisk P. Eur Polym J 1995;31:1269.
[32] Capek I, Potisk P. Macromol Chem Phys 1995;196:723.
[33] Capek I, Potisk P. J Polym Sci Polym Chem Ed 1995; 33:1675.
[34] Escalante JI, Rodríguez-Guadarrama LA, Mendizábal E, Puig J, López RG, Katime I. J Appl Polym Sci 1996;62: 1313.
[35] López RG, Treviño ME, Salazar LV, Peralta RD, Becerra F, Mendizábal E, Puig JE. Polym Bull 1997;38:411.
[36] Morgan JD, Lusvardi KL, Kaler EW. Macromolecules 1997;30:1897.
[37] Capek I, Juranicová V, Barton J, Asua JM, Ito K. Polym Int J 1997;43:1.
[38] Xu X, Zhang Z, Wu H, Ge X, Zhang M. Polymer 1998; 39:5245.
[39] Sosa N, López RG, Peralta RD, Katime I, Becerra F, Mendizábal E, Puig JE. Macromol Chem Phys 1999; 200:2416.
[40] Sosa N, Zaragoza EA, López RG, Peralta RD, Katime I, Becerra F, Mendizabal E, Puig JE. Langmuir 2000;16: 3612.
[41] Rabelero M, Zacarías M, Mendizábal E, Domínguez JM, Katime I. Polym Bull 1997;38:695.
[42] Ming W, Jones FN, Fu SK. Polym Bull 1998;40:749.
[43] Ming W, Jones FN, Fu S. Macromol Chem Phys 1999; 199:1075.
[44] Xu XJ, Chew CH, Siow KS, Wong MK, Gan LM. Langmuir 1999;15:8067.
[45] Hammond GS, Newman RC. J Am Chem Soc 1963;85: 1501.
[46] Bleger F, Murthy AK, Pla F, Kaler EW. Macromolecules 1994;27:2559.
[47] Bovey FA, Kolthoff IM. J Am Chem Soc 1947;69: 1501.